Characterization of the Metal Receptor Sites in *Escherichia coli* Zur, an Ultrasensitive Zinc(II) Metalloregulatory Protein†

Caryn E. Outten,‡ Daniel A. Tobin,§ James E. Penner-Hahn,§ and Thomas V. O'Halloran*,‡,||

Department of Chemistry and Department of Biochemistry, Molecular Biology, and Cell Biology, Northwestern University, Evanston, Illinois 60208, and Department of Chemistry, University of Michigan, Ann Arbor, Michigan 48109

Received May 14, 2001; Revised Manuscript Received July 23, 2001

ABSTRACT: The *Escherichia coli* Zur protein is a Fur homologue that regulates expression of Zn(II) uptake systems. The zinc-loaded form of Zur is proposed to bind DNA and repress transcription of the *znuABC* genes. Recent in vitro data indicate that the transcriptional activity of Zur is half-maximal when free Zn(II) concentrations are in the sub-femtomolar range, making it the most sensitive Zn(II) metalloregulatory protein reported to date. Previous results indicate that Zur binds at least one zinc; however, little else is known about Zn(II) binding. We have purified *E. coli* Zur to homogeneity and found that it has two Zn(II) binding sites per monomer with different coordination environments. Using Zn(II) binding assays, ICP-AES analysis, and Zn EXAFS analysis, we show that one zinc is tightly bound in an $S_3(N/O)$ coordination environment. Both Co(II) and Zn(II) were substituted into the second metal binding site and probed by EXAFS and UV−visible absorption spectroscopy. These studies indicate that Co(II) is bound in an $S(N/O)_3$ coordination environment with tetrahedral geometry. The Zn(II) EXAFS of Zn_2Zur, which is consistent with the results for both sites, indicates an average coordination environment of $S_2(N/O)_2$, presumably due to one $S(N/O)_3$ site and one $S_3(N/O)$ site. These studies reveal the coordination environments that confer such exceptional zinc sensitivity and may provide the foundation for understanding the molecular basis of metal ion selectivity. A comparison of the metal binding sites in Zur with its Fe(II)-sensing homologue Fur provides clues as to why these two proteins with similar structures respond to two very different metal ions.

Zinc plays many critical roles in cell metabolism, but elevated concentrations of this metal have severe detrimental effects. Consequently, the processes of Zn(II) uptake, storage, deployment, and export, known collectively as Zn(II) homeostasis, are essential activities for all organisms. Zn(II)-sensing metalloregulatory proteins are at the center of these homeostasis systems. Zinc has several qualities that distinguish it from other transition metals. It is a strong Lewis acid with no redox activity under physiological conditions, and coordinated water can undergo rapid ligand exchange. For these reasons, it is an excellent cofactor for catalytic enzymes that provide an unsaturated coordination sphere. Although zinc bonds can be kinetically labile, zinc chelate complexes also tend to be thermodynamically stable. Therefore, with a saturated coordination environment, zinc can serve as a scaffold that maintains the proper folded structure of a protein.

Bacteria have developed both uptake and export systems that work together to maintain the proper levels of zinc in the cell. In *Escherichia coli*, expression of these systems is controlled at the transcriptional level by the metalloregulatory proteins ZntR (*1*−*3*) and Zur (*4*, *5*). These regulators sense zinc concentrations in the cell and then repress Zn(II) uptake systems (Zur) or activate Zn(II) export systems (ZntR) accordingly. The protein examined in this study, Zur, is a member of the Fur family of bacterial metal-responsive regulators. Genetic studies indicate that the *zur* gene is essential for the Zn(II)-dependent repression of the Zn(II) uptake system, *znuABC* (*4*). In vitro studies show that Zn-Zur binds specifically to a 30 bp region located between the divergently transcribed *znuCB* and *znuA* genes and represses transcription of this operon (*5*, *6*). Zur is reported to be a dimer in its native form and binds at least one zinc ion per monomer (*5*).

Fur, the Fe(II)-sensing homologue of Zur, binds one zinc ion per monomer in an $S_2(N/O)_2$ environment (*7*, *8*). Fur and Zur are 27% identical in amino acid sequence, and it is not clear why they both bind Zn(II) since they respond to different metal ions in vivo. The Zn(II) ion in Fur may function physiologically as a structural cofactor since it is essential for DNA binding and protein stability and is very difficult to remove from the protein (*7*), although regulatory roles for Zn(II) occupancy cannot be ruled out. Binding of Fe(II) to Fur does not displace the Zn(II) ion (*7*); rather, Fe(II) binds in a different site with five or six N/O ligands (*9*). On the basis of chemical modification and mass spectrometry analysis, cysteine residues located at positions 93 and 96 are proposed to coordinate the Zn(II) ion in Fur

† This research has been supported in part by NIH Research Grants T32 GM08382 (to C.E.O.), R01 GM38784 (to T.V.O.), and R01 GM38047 (to J.E.P.-H).

* To whom correspondence should be addressed. Phone: 847-491-5060. Fax: 847-491-7713. E-mail: t-ohalloran@northwestern.edu.

‡ Department of Chemistry, Northwestern University.

§ Department of Chemistry, University of Michigan.

|| Department of Biochemistry, Molecular Biology, and Cell Biology, Northwestern University.

10.1021/bi0155448 CCC: $20.00 © xxxx American Chemical Society
Published on Web 00/00/0000 PAGE EST: 6.7

(*8*). To date, biochemical repression by iron-bound forms of *E. coli* Fur has not been demonstrated in vitro, so the regulation mechanism remains an open issue.

In vitro studies of the Zur protein indicate that it binds DNA and represses transcription in vitro in a Zn(II)-responsive manner. Furthermore, the results reveal that this sensor has the highest Zn(II) affinity reported for a Zn(II) protein: Zur repression of the *znuC* gene is triggered by subfemtomolar ($<10^{-15}$) levels of free Zn(II) (*6*). This value, which is derived from activity assays, corresponds to the concentration of free Zn(II) ion that gives half-maximal repression in vitro. When viewed as a Zn(II)-Zur binding constant, it represents the tightest known Zn(II) binding constant for a native protein. Zinc fingers, in comparison, have measured dissociation constants ranging from 10^{-8} to 10^{-15} M (*10*−*14*).

To understand the molecular basis of this extraordinary sensitivity for Zn(II), we have initiated a series of biochemical and spectroscopic studies of the Zn-bound forms of Zur. The results indicate that, like Fur, Zur also has two distinct metal binding sites. One site, which is functionally analogous to the Zn(II) site in Fur, binds Zn(II) in an S_3(N/O) coordination environment. Like Fur, the Zn(II) ion is difficult to displace from this site. The second site, from which zinc is more easily exchanged, binds Zn(II) or Co(II) in a tetrahedral $S(N/O)_3$ coordination environment. A study of the metal binding sites in Zur and comparison of Zur to Fur are useful for establishing how metal sensors selectively recognize their target metals.

EXPERIMENTAL PROCEDURES

Plasmid Construction, Bacterial Strains, and Materials. All DNA manipulations were carried out using standard procedures (*15*). Plasmid construction was confirmed by DNA sequencing, and all cloning was carried out in the *E. coli* strain DH5α. All chromatography resins and columns were purchased from Amersham Pharmacia Biotech. All buffers used in preparing samples for EXAFS[1] and UV−visible spectroscopy were treated with Chelex-100 resin (Bio-Rad) overnight to remove trace metals.

Zur Cloning and Purification. The *zur* gene was amplified from the *E. coli* chromosome using primers Zur N-terminal (5′-CTT TGA GGT GCC CCA TGG AAA AGA CCA C-3′) and Zur C-terminal (5′-GTG TAC AAG GAT CCA CGC CCT CTT AAC G-3′). The 554 bp PCR fragment was digested with *Nco*I and *Bam*HI and inserted into pET24d (Novagen) digested with the same enzymes. The resulting overexpression vector (pET24dZur) was transformed into BL21(DE3) (Novagen). The cells were grown in 10 L of LB media with shaking at 37 °C and induced with 400 μM IPTG when $OD_{600} = 0.6$. The cells were harvested by centrifugation 2.5 h after induction and then stored at −80 °C. Following sonication, the cell pellet was resuspended in 100 mL of extraction buffer (20 mM Tris-HCl, pH 8.0, 6 M urea, 100 mM DTT) in order to extract the Zur protein. The solubilized protein was then refolded by dropping the urea extract slowly into 2 L of refolding buffer (20 mM Tris-HCl, pH 8.0, 100 μM $ZnSO_4$, 5 mM DTT) at 4 °C with stirring. The presence of Zn(II) in the refolding buffer was found to prevent precipitation of the protein and improve the yield of the purification. The protein was then loaded onto a DEAE-Sepharose Fast Flow column equilibrated with 20 mM Tris-HCl, pH 8.0, and 5 mM DTT and eluted with a salt gradient. Ammonium sulfate was added to the pooled Zur protein fractions to a final concentration of 1 M, and the protein was loaded onto a phenyl-Sepharose high-performance hydrophobic column equilibrated with 50 mM Tris-HCl, pH 8.0, 1 M $(NH_4)_2SO_4$, and 5 mM DTT. The protein was eluted with a decreasing salt gradient, and the Zur-containing fractions were pooled and concentrated to ∼2 mL. The protein was then loaded onto a High-Load Superdex 75 gel filtration column equilibrated with buffer A (50 mM Tris-HCl, pH 8.0, 250 mM NaCl, 5 mM DTT). Zur was concentrated to 1−2 mL and showed one band on overloaded SDS−PAGE gels. Protein was stored at −80 °C in buffer A with 5% glycerol.

Protein−Metal Ratio Determination. A calculated extinction coefficient for Zur ($\epsilon_{280} = 4380\ M^{-1}\ cm^{-1}$) (*16*) in 20 mM Mes, pH 6.0, and 6 M guanidine hydrochloride was used to standardize the Bradford assay (Bio-Rad) with IgG as the calibration standard. The Bradford assay was found to overestimate the Zur concentration by 2.33 in comparison to the extinction coefficient. With this correction factor, protein concentration was routinely determined by the Bradford assay. Metal concentrations were determined by inductively coupled plasma atomic emission spectroscopy (ICP-AES) using a Thermo Jarrell Ash AtomScan 25 ICP-AE spectrometer.

Zn(II) Removal from Zur. Zur, as purified above, typically contained 1.4−1.8 mol of Zn(II)/mol of Zur monomer. To prepare Zn_1Zur, 100−500 μM purified Zur was incubated overnight at 4 °C in buffer A with 500 μM TPEN or 50 mM EDTA. The protein was then exchanged into buffer without chelator for metal analysis. This procedure typically yielded 1.0 ± 0.2 Zn per Zur monomer. Complete removal of zinc from Zur required treatment with urea combined with extensive incubation with TPEN. To make apo-Zur, 30 μM Zur was stirred at 4 °C for 48 h in an Amicon ultrafiltration cell containing buffer A with 6 M urea and 500 μM TPEN. The buffer was exchanged three times during the experiment (50:1 dilution each time).

Co(II),Zn-Zur UV−Visible Absorption Spectroscopy. Co(II),Zn-Zur was prepared by first making Zn_1Zur as described above. The protein was then transferred to an inert atmosphere at 10 °C and exchanged into Hepes buffer (50 mM Hepes, pH 8.0), and 2 equiv of Co(II) was added with stirring in an Amicon ultrafiltration cell. After removal of unbound metal, the protein contained 0.8 mol of Zn(II) and 0.9 mol of Co(II) per Zur monomer. This sample was sealed in an anaerobic cuvette at a final protein concentration of 145 μM. The absorption spectrum from 250 to 800 nm was obtained at room temperature using a Varian Cary Bio 300

[1] Abbreviations: EXAFS, extended X-ray absorption fine structure; bp, base pair; PCR, polymerase chain reaction; IPTG, isopropyl β-D-thiogalactopyranoside; Tris, tris(hydroxymethyl)aminomethane; DTT, DL-dithiothreitol; XANES, X-ray absorption near edge structure; DEAE, diethylaminoethyl; Mes, 2-(*N*-morpholino)ethanesulfonic acid; Hepes, *N*-(2-hydroxyethyl)piperazine-*N*′-2-ethanesulfonic acid; ICP-AES, inductively coupled plasma atomic emission spectroscopy; TPEN, *N*,*N*,*N*′,*N*′-tetrakis(2-pyridylmethyl)ethylenediamine; EDTA, ethylenediaminetetracetic acid; FT, Fourier transform; BVS, bond valence sum.

UV−visible spectrophotometer. Zn(II) was added anaerobically to Co(II),Zn-Zur in 0.1 mol equiv steps, allowing 10 min for the sample to equilibrate after each Zn(II) addition. The spectra were recorded using Zn_1Zur as a blank and were corrected for dilution.

Preparation of Zn_1Zur, Zn_2Zur, and Co(II),Zn-Zur EXAFS Samples. All EXAFS samples were prepared in an inert atmosphere, transferred to an EXAFS cuvette (Lucite body, Kapton windows), and then immediately frozen in liquid N_2. Zn_2Zur was prepared by exchanging the purified protein into buffer containing 100 mM Tris−Mes, pH 8.0, and 30% glycerol. The protein concentration was 9.6 mM with 1.8 mol of Zn per Zur monomer. Zn_1Zur was prepared as described above and then exchanged into phosphate buffer (50 mM sodium phosphate, pH 8.0) with 30% glycerol. The protein concentration was 1.5 mM with 1.3 mol of Zn per Zur monomer. Co(II),Zn-Zur was prepared in a manner similar to the electronic spectroscopy sample; however, the protein was exchanged into phosphate buffer prior to Co(II) addition. The unbound metal was washed away with three buffer exchanges (50:1 dilutions), and glycerol was added to a final concentration of 30%. The protein concentration was 1.6 mM with 1.2 mol of Zn(II) and 0.9 mol of Co(II) per Zur monomer.

X-ray Absorption Spectroscopy and Data Analysis. X-ray absorption spectra were measured at the Stanford Synchrotron Radiation Laboratory (SSRL) on beam line 9-3 using a Si(220) double crystal monochromator with a Rh-coated mirror upstream of the monochromator used for harmonic rejection. The storage ring operated under normal conditions (3.0 GeV, 60−100 mA). Incident intensity was measured with a N_2-filled ion chamber. Energies were calibrated using the absorption spectrum of a zinc foil or a cobalt foil that was collected concurrently with each sample. Edge energies were defined using the first inflection point of the zinc foil spectrum (9659 eV) or the cobalt foil spectrum (7709 eV). The sample temperature was held at approximately 10 K using an Oxford liquid helium flow cryostat. Fluorescence excitation spectra were collected using a 30-element Ge solid-state detector array with the exception of one sample that was collected using an Ar-filled fluorescence ion chamber (Zn_2Zur). The total integrated count rates were held below 110 kHz/channel to avoid saturation, giving an average Zn Kα fluorescence count rate of 34 kHz and a Co Kα fluorescence count rate of 10 kHz. Each scan had 10 eV increments in the preedge region, 0.35 eV increments in the edge region, and 0.05 $Å^{-1}$ increments in the EXAFS region. Integration times were 1 s in preedge and edge regions and 1−20 s k^3-weighted in the EXAFS region for a total scan time of ∼35 min. Each detector channel of every scan (four to seven scans per sample) was checked for glitches, and the good channels (24 to 25) were averaged for each sample to yield the final spectrum.

The XANES data were normalized to tabulated X-ray absorption cross sections by fitting a polynomial to regions both below and above the edge with a single second-order polynomial and a single scale factor. The EXAFS background correction was performed by fitting a polynomial to the preedge region and a two-region cubic spline to the postedge region (zinc spline points, 9675, 9900, 10270; cobalt spline points, 7745, 7980, 8420). The data were then converted to k-space using eq 1 where E_0 is 9675 eV for zinc and 7725 eV for cobalt.

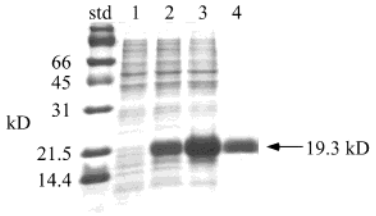

FIGURE 1: SDS−PAGE gel from Zur purification procedures: std, molecular mass standards; lane 1, uninduced cells; lane 2, induced cells; lane 3, urea extract; lane 4, 15 μg of purified Zur.

$$k = \sqrt{\frac{2m_e(E - E_0)}{\hbar^2}} \quad (1)$$

Fourier transforms were calculated using k^3-weighted data over a range of 2−12.3 $Å^{-1}$ for zinc and 2.2−12.6 $Å^{-1}$ for cobalt. Data were fit using the data analysis protocol described previously (*17*) for determining Zn ligation (see Figure S1, Supporting Information). FEFF version 6.01 (*18*) was used to generate phase and amplitude functions for Zn−S, Zn−N, Co−N, and Co−S absorber−scatterer pairs. The Zn data were calibrated as described previously (*17*). The optimized scale factor and ΔE_0 for Co−N (0.8 and 5, respectively) were determined by fitting EXAFS data for (*meso*-tetraphenylporphorinato)cobalt (II). The same ΔE_0 and a scale factor 1.0 were used for Co−S. For Co fits, the total coordination number was held constant at either 4 or 5, based on the observed Co−ligand bond lengths, which are too short to be compatible with a 5-coordinate Co(II). In the fits, the *N* and *S* coordination numbers were fixed at integer values, and only R_{as} and σ^2 were allowed to vary.

The area of the 1s → 3d transition in the normalized Co XANES spectrum was isolated either by fitting a background function (linear + arctan) to the region below (7700−7707 eV) and above (7714−7719 eV) the transition or by fitting a background function (linear + arctan) and a Gaussian function to the entire preedge region (7000−7719 eV). The 1s → 3d area was determined by numerical integration and gave similar results for either method.

RESULTS

Zur Purification and Metal Content. Figure 1 shows an SDS−PAGE gel of different steps in the Zur purification process. A 10 L preparation typically yielded ∼85 mg of pure protein containing 1.4−1.8 mol of Zn(II) per monomer. Treatment with strong Zn(II) chelating agents alone left 1 equiv of Zn(II) still bound to the protein. Urea denaturation of the protein coupled with extensive incubation with chelating agents was necessary to remove almost all of the zinc from the protein. Even after this treatment, 0.1 mol of Zn(II) (per mol of Zur monomer) still remained in the protein.

Co(II),Zn-Zur Electronic Absorption Spectroscopy Analysis. Substitution of Co(II) into one of the Zn(II) binding sites in Zur provides a useful handle to study the protein by UV−visible absorption spectroscopy. The absorption spectrum of Co(II),Zn-Zur is shown as a bold line in Figure 2. The thinner lines are the resulting spectra after each addition of 0.1 mol equiv of $ZnSO_4$ up to 1.0 mol equiv total. The protein started to precipitate out of the solution upon the addition of 1.1

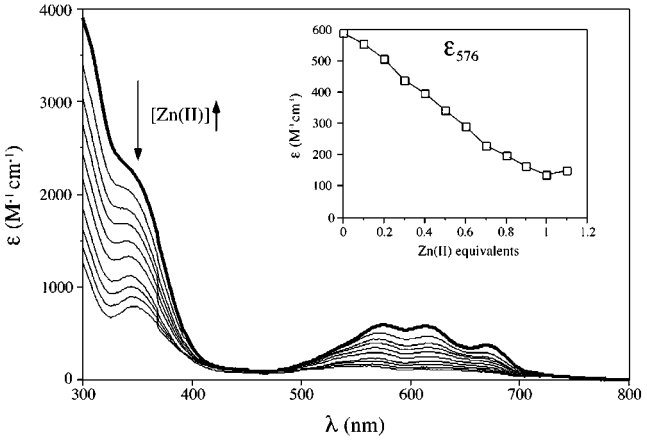

FIGURE 2: Electronic absorption spectra of Co(II),Zn-Zur anaerobically titrated with 0−1.0 equiv of Zn(II). The sample contains 145 μM Zur in 50 mM Hepes, pH 8.0. The solid line is the spectrum of Co(II),Zn-Zur before displacement of the Co(II) with Zn(II). The thinner lines are the spectra after each addition of Zn(II). Inset: Absorption change at 576 nm as a function of added Zn(II). The full-scale absorption of the Co(II),Zn-Zur corresponds to 0.086 AU, and the ϵ is reported per protein monomer.

total mol equiv. Since all of the absorption bands decrease in intensity linearly with the addition of Zn(II), it is apparent that Co(II) is being substituted by the spectroscopically silent Zn(II) ion. Three distinct bands are evident in the 500−700 nm range corresponding to the d−d transitions of Co(II). The band with maximum absorption in this region is located at 576 nm (ϵ = 590 M^{-1} cm^{-1}), while the other bands are located at 614 (ϵ = 580 M^{-1} cm^{-1}) and 670 nm (ϵ = 370 M^{-1} cm^{-1}). Co(II) d−d transitions in this region with extinction coefficients >300 M^{-1} cm^{-1} are hallmarks for tetrahedral coordination. Pentacoordinate Co(II) sites have weaker absorptivities (50 < ϵ < 250 M^{-1} cm^{-1}), while octahedral sites are even lower (ϵ < 30 M^{-1} cm^{-1}) (*19*). The number of sulfur ligands affects the energy of these d−d transitions. The more sulfurs that are coordinated to the Co(II) ion, the lower the energy of the given transition. The energies of the d−d transitions for Co(II)-Zur are most consistent with $S(N/O)_3$ coordination (*20*−*22*), although $S_2(N/O)_2$ cannot be completely ruled out.

The intense absorption band located at 350 nm (ϵ = 2300 M^{-1} cm^{-1}) also supports an $S(N/O)_3$ model for Co(II) coordination. This band is characteristic of thiolate → Co(II) ligand-to-metal charge transfer. The magnitude of this band is correlated to the number of thiolate ligands coordinated to the Co(II) ion. The difference in intensity of this band between 0 and 1.0 mol equiv of added Zn(II) is 1450 M^{-1} cm^{-1}. Literature values for Co−S absorption in this near-ultraviolet region vary from 900 to 1400 M^{-1} cm^{-1} per thiolate−cobalt bond (*22*−*25*). Therefore, this band most likely reflects the presence of one sulfur−cobalt bond. The remaining absorbance at 350 nm after the addition of 1.0 mol equiv of Zn(II) (ϵ = 850 M^{-1} cm^{-1}) may be caused by a small amount of Co(II) binding in the other, slowly exchanging Zn(II) binding site.

Zn(II) and Co(II) EXAFS Analysis. Three samples of Zur protein were measured: Zur with 1 Zn per monomer (Zn_1Zur), Zur with 2 Zn per monomer (Zn_2Zur), and Zur with one Zn per monomer and one Co per monomer [Co(II),-Zn-Zur]. The Zn(II) XAS data are shown in Figures 3A and

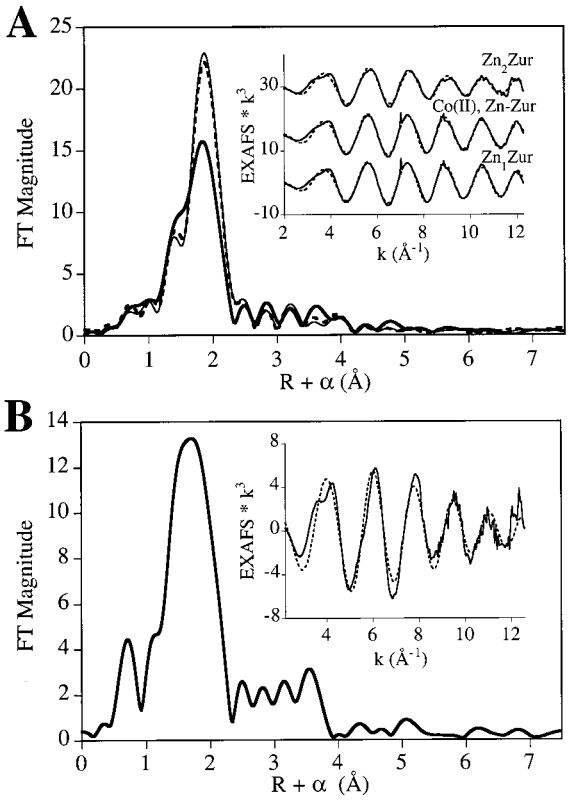

FIGURE 3: Fourier transforms and k^3-weighted Zn and Co EXAFS for all three Zur protein samples. (A) Fourier transform of Zn EXAFS. The thin solid line (—) is Zn_1Zur, the dashed line (- - -) is Co(II),Zn-Zur, and the thick solid line (**—**) is Zn_2Zur. Inset: k^3-weighted EXAFS data, shown as a solid line (—), overlaid with the best fit [$S_3(N/O)$ for Zn_1Zur and Co(II),Zn-Zur, $S_2(N/O)_2$ for Zn_2Zur] shown as a dashed line (- - -). (B) Fourier transform and k^3-weighted Co EXAFS for Co(II),Zn-Zur. The inset shows the k^3-weighted EXAFS as a solid line (—) overlaid with the best fit [$S(N/O)_3$] shown as a dashed line (- - -).

4A, while the Co(II) XAS data are shown in Figures 3B and 4B. Although the Zn_1Zur Fourier transform (FT) height and symmetry indicate a zinc coordination environment that is dominated by sulfur (Figure 3A), several lines of evidence demonstrate that the site has some nitrogen/oxygen ligation. The best fit (Table 1) is consistent with a coordination environment of $S_3(N/O)$ for Zn_1Zur. In particular, the improvement in fit quality between the ZnS_4 fit and the $ZnS_3(N/O)$ fit is larger than is seen for authentic ZnS_4 samples (*17*). In addition, the Zn−S bond length is shorter than those found for authentic tetrathiolate sites. Finally, only the $S_3(N/O)$ fit for Zn_1Zur gives Debye−Waller factors similar to those found in model compounds. Alternative models (e.g., a 5-coordinate Zn site) can be ruled out on the basis of the observed bond lengths; these are consistent with a 4-coordinate site and too short for a 5-coordinate site, as confirmed by bond−valence−sum (BVS) calculations (*26*).

To independently evaluate the two metal sites in Zur, a mixed metal sample was made using zinc and cobalt [Co(II),-Zn-Zur]. The zinc EXAFS results were identical to those for Zn_1Zur (see Table 1), indicating that the Zn_1Zur sample represents a homogeneous population in which the single Zn(II) ion is bound in a specific site. In other words, this indicates that the zinc in Co(II),Zn-Zur resides solely in one metal binding site and that this site is the same as that found in Zn_1Zur.

Table 1: Zur EXAFS Fitting Results for Filtered Data

sample	N^a	R (Å)	σ^2 (Å^2 × 10^{-3})	N^a	R (Å)	σ^2 (Å^2 × 10^{-3})	F'^b	BVS^c
Zn_1Zur				4S	2.325	4.6	0.021	2.4
	1N	2.068	8.4	3S	2.327	2.8	0.018	2.3
	2N	2.088	5.5	2S	2.331	0.7	0.036	2.1
	3N	2.136	3.6	1S	2.335	0.0	0.173	1.8
Zn_2Zur				4S	2.304	7.5	0.042	2.5
	1N	2.023	1.9	3S	2.310	4.7	0.025	2.4
	1.75N	2.040	3.6	2.25S	2.315	3.0	0.019	2.3
	2N	2.044	3.8	2S	2.316	2.4	0.019	2.3
	3N	2.069	5.4	1S	2.320	0.0	0.050	2.1
Co,**Zn**-Zur[d]				4S	2.324	4.8	0.023	2.4
	1N	2.049	6.2	3S	2.327	2.9	0.014	2.3
	2N	2.077	5.4	2S	2.330	0.7	0.026	2.1
	3N	2.127	4.5	1S	2.333	0.0	0.156	1.9
Co,Zn-Zur[d]	5N	2.082	5.9				0.167	2.3
	4N	2.084	4.5				0.175	1.9
	4N	2.060	7.0	1S	2.285	1.7	0.050	2.6
	3N	2.049	3.2	1S	2.294	0.4	0.031	2.2
	3N	2.096	9.3	2S	2.261	6.1	0.058	2.7
	2N	2.059	4.5	2S	2.279	5.2	0.063	2.3

[a] Number of scatterers in the fit. [b] Goodness of fit weighted by the number of free variables: $F' = [k^6(\text{data} - \text{fit})^2]/(N_{ind} - N_{var})$, where $N_{ind} = [2(\Delta k)(\Delta R)]/\pi$ is the number of independent data points and N_{var} is the number of variable parameters. [c] BVS calculated using the procedure in ref *25* using nitrogen for the low-Z ligand. [d] The metal in bold for the Co,Zn-Zur fits indicates the metal to which the fit corresponds.

In contrast, the Fourier transform of the EXAFS data for Zn_2Zur (Figure 3A) suggests that the second Zn has a very different structure. The lower amplitude and significant asymmetry of the FT indicate a significant increase in the fraction of N/O ligation. Curve fitting results (Table 1) are somewhat more difficult to interpret, since these data represent the average of two different zinc sites. The best integer fit is found for two sulfur and two low-Z ligands, indicating that the second Zn must have primarily low-Z ligands. If the second Zn site had *all* low-Z ligands, then the average structure for Zn_2Zur would be $ZnS_{1.5}N_{2.5}$; the presence of a single thiolate bound to the second Zn would give an average structure of ZnS_2N_2. The best fit, allowing noninteger coordination numbers, gives $ZnS_{1.75}N_{2.25}$, which would be consistent with either possibility. However, given the evidence (above) for thiolate ligation to Co(II) when it is bound in the second Zn site, it is most likely that the second Zn site has $ZnS(N/O)_3$ ligation. Once again, the observed bond lengths, or, alternatively, the calculated bond−valence−sums, are consistent with both of the Zn sites being 4-coordinate.

The first shell FT peak width and asymmetry of Co(II) in Co(II),Zn-Zur suggest the presence of two shells of nearest neighbors (Figure 3B). In studies of model compounds, such obviously split peaks are only observed when the low-Z ligand is the majority ligand (*17*). This is because the sulfur EXAFS is inherently more intense than the low-Z EXAFS and thus tends to dominate the Fourier transform if there are two or more sulfur ligands. Consistent with this, the Co EXAFS is best fit using only a single sulfur ligand (Table 1). Attempts to include more sulfurs give fits that are 2-fold worse, and Debye−Waller factors are larger than expected (*17*). The two best fits are for $CoS(N/O)_3$ and $CoS(N/O)_4$. The $CoS(N/O)_3$ fit has the best fit quality and gives the most reasonable bond−valence−sum; however, the $CoS(N/O)_3$ fit gives a Debye−Waller factor that is quite small. Nevertheless, the area of the 1s → 3d transition (inset to Figure 4B) is 15 × 10^{-2} eV, which is compatible with a 4-coordinate Co but larger than expected for a 5-coordinate Co (*27*). Since the area of the 1s → 3d transition and the intensity of the Co d−d bands in the visible spectrum both depend on 3d + 4p orbital mixing, it is gratifying that both point to a 4-coordinate Co(II) site. Considering all of the data, we favor a $CoS(N/O)_3$ structure for this site, although a $CoS_2(N/O)_2$ site cannot be completely excluded. The smaller than expected Debye−Waller factor for the Co−S shell probably reflects uncertainty in the Co−S scale factor, due to the lack of a Co−S reference compound.

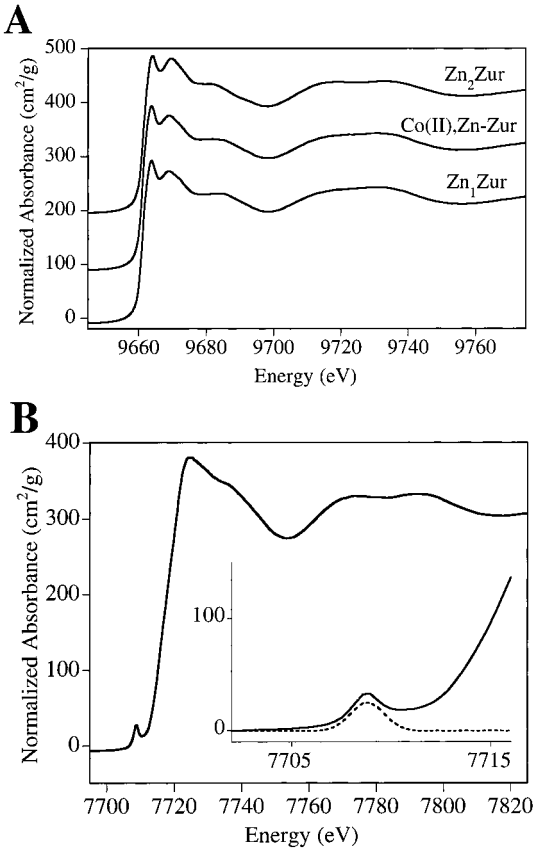

FIGURE 4: Normalized Zn and Co XANES spectra of Zur. (A) Normalized Zn XANES spectra of Zur samples. Spectra are plotted on the same scale and offset vertically for clarity. (B) Normalized Co XANES spectrum of the Co(II),Zn-Zur sample. Inset: Expansion of 1s → 3d transition (solid); background removed 1s → 3d transition (dashed).

DISCUSSION

Zur is typically isolated with 1 or 2 Zn(II) atoms per monomer. The question arises whether two thermodynamically and structurally distinct sites can be characterized. Taken together, the ICP-AES, EXAFS, and UV−visible spectroscopy data indicate that Zur does have two distinct Zn(II) binding sites. One site, which we will call site A, binds Zn(II) very tightly and is difficult to substitute with other metals. For this reason, Co(II) could not be used to probe site A since apo-Zur will preferentially bind exogenous Zn(II) in the buffer rather than other metals added in excess. The same problem is encountered when trying to substitute metals into site A in Fur (*7*). The coordination environment of site A, $S_3(N/O)$, does not change upon binding a second

(A)

```
Zur   1 MEKTTTQELLAQAEKICAQRNVRLTPQRLEVLRLMSLQDG.AISAYDLLDLLREAEPQA
          |   |  |      :::|  ||::| ::    |   :|| ||   | :   :
Fur   1 MTDNNTA--LKKAG-------LKVTLPRLKILEVLQEPDNHHVSAEDLYKRLIDMGEEI

Zur  59 KPPTVYRALDFLLEQGFVHKVESTNSYVLCHLFDQPTHTSAMFICDRCGAVKEECAEGV
          |||| |:   : | | :       :  |  |  |     ||  || | |   : :
Fur  51 GLATVYRVLNQFDDAGIVTRHNFEGGKSVFELTQQHHHDH..LICLDCGKVIEFSDDSI

Zur 118 EDIMHTLAAKMGFALRHNVIEAHGLCAACVEVEACRHPEQCQHDHSVQVKKKPR 171
          |    :||| |  |     :  |   | | : ||       :|:   |
Fur 108 EARQREIAAKHGIRLTNH---SLYLYGHCAEGD-CR-----EDEHAHEGK     148
```

(B)

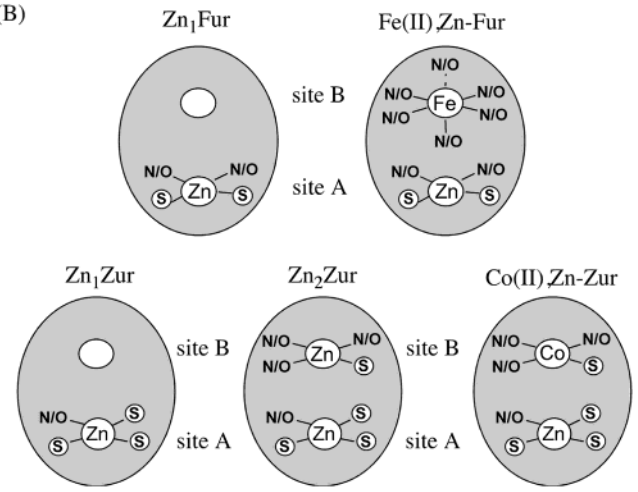

FIGURE 5: Metal binding site comparison of Fur and Zur. (A) Amino acid alignment of the *E. coli* Fur and Zur proteins. Identical amino acids are indicated by a vertical line (|), while similar residues are shown with a colon (:). The two Zn(II) binding cysteine residues of Fur that are conserved in Zur are shown in bold. (B) Models of the metal binding sites in Zn_1Fur, Fe(II),Zn-Fur, Zn_1Zur, Zn_2Zur, and Co(II),Zn-Zur.

metal ion in the other site (site B). On the other hand, site B can bind either Co(II) or Zn(II) specifically and is more readily exchangeable. The affinity of site B for Zn(II) is greater than its affinity for Co(II), since Zn(II) easily displaces Co(II) in titration experiments. The Co(II) absorption spectrum of Co(II),Zn-Zur indicates a tetrahedral $S(N/O)_3$ or $S_2(N/O)_2$ environment for Co(II), ruling out a pentacoordinate site, and this is confirmed by the 1s → 3d transition. The Co(II) EXAFS indicates $S(N/O)_3$ or $S(N/O)_4$ coordination, ruling out an $S_2(N/O)_2$ site. Since the EXAFS and UV−visible spectroscopy samples were prepared in slightly different buffers, a portion of the Co(II),Zn-Zur EXAFS sample was examined by UV−visible spectroscopy. The spectrum of this sample looked identical to that in Figure 2, which leads to the conclusion that coordination of Co(II) is the same for both sample conditions. Therefore, combining the EXAFS and electronic absorption spectroscopy results, we conclude that the Co(II) binds in an $S(N/O)_3$ environment. The EXAFS data for Zn_2Zur is consistent with the second Zn(II) ion binding in an $S(N/O)_3$ environment as well.

A comparison of the amino acid sequences and metal binding sites of Fur and Zur highlights a few similarities and some important differences between the two proteins (Figure 5). The two Zn(II) binding cysteines in Fur (Cys-93 and Cys-96) are conserved in Zur as well as most other Fur/Zur homologues in other bacteria (*5*). This zinc ion in Fur is very difficult to remove, as is one of the zinc ions in Zur. Therefore, it is reasonable to propose that the equivalent cysteines in Zur (Cys-103 and Cys-106) bind Zn(II) in the tight binding site (site A). This zinc is proposed to play a structural role in Fur (*7*, *28*) as may be the case with Zur. As a structural cofactor, the zinc ion could be buried in the protein interior, lacking contact with the buffer solution. This would explain the difficulty encountered in attempting to remove Zn(II) from site A in either Fur or Zur. However, the tight Zn(II) binding sites in Fur and Zur (sites A) are not identical—the Fur site is reported to be $S_2(N/O)_2$ with at least one histidine, while the Zur site is $S_3(N/O)$. This difference may reflect the ratio of cysteines vs histidines in each protein: Fur has 12 histidines and only 4 cysteines out of 148 amino acids, while Zur has 9 cysteines and 9 histidines out of 171 amino acids. It will be interesting to compare the zinc affinities and kinetics for the Fur and Zur structural zinc sites.

Despite the subtle differences between the structural Zn(II) sites in Fur and Zur, the question still remains: how do Fur and Zur selectively respond to either Fe(II) or Zn(II)? A comparison of site B in both proteins provides a potential answer to this question. The second metal binding site in Zur (site B) binds zinc in an $S(N/O)_3$ site. This coordination environment is markedly different from the Fe(II) binding site in Fur (site B), which has five or six N/O ligands. These differences are significant when considering the thermodynamics of metal binding for Fe(II) vs Zn(II). Since Zn(II) is a d^{10} metal ion, it is not subject to ligand field stabilization effects. Therefore, it can bind in a tetrahedral site without a loss in ligand field stabilization energy. Fe(II), on the other hand, is a d^6 metal ion, so tetrahedral coordination is thermodynamically unfavorable in relation to octahedral or pentacoordination. On the basis of these arguments, it is possible that site B in Fur functions to recognize Fe(II), while in Zur it specifically favors Zn(II).

It is unlikely that site A is the sensor site since overnight incubation with 500 μM TPEN alone cannot remove this zinc ion from the protein. The protein must first be unfolded with urea. TPEN does, however, abolish Zur DNA binding activity at 25 μM concentration after a 30 min incubation in footprinting experiments (*6*). Footprinting experiments in that study were conducted with Zn_1Zur, although the exact form of the protein binding the DNA cannot be known since Zur can bind exogenous Zn(II) in the footprinting buffer. For this reason a strong Zn(II) chelator is required to examine Zn(II) binding. Site A is probably occupied under these DNA binding conditions, implying that site B is the sensor site. At this point, however, we cannot rule out the possibility that site A is the only site occupied in vivo, and thus the metal-sensing site. In fact, the two sites may work together to ensure rapid equilibration of Zn(II) with other components of Zn(II) homeostasis systems. The free zinc concentration required to activate Zur has been measured in vitro as 2.0×10^{-16} (*6*). In the future, a quantitative analysis of the metal binding affinity of each zinc site in Zur may reveal which site is the Zn(II) sensor site.

Understanding the molecular basis of metal ion recognition and selectivity for Zur is key to exploring the bioinorganic chemistry of zinc. It is interesting to note that the proposed metal-sensing site in Zur (site B) is very similar to the sensor site in another Zn(II) metalloregulatory protein, SmtB from *Synechococcus* PCC7942. SmtB regulates Zn(II) homeostasis in this cyanobacterium by repressing expression of SmtA, a metallothionein that functions in Zn(II) sequestration (*29*).

Spectroscopic characterization of the metal binding site of SmtB was recently reported by VanZile et al. (*22*). They found that both Zn(II) and Co(II) bind to SmtB in a tetrahedral environment with $S(N/O)_3$ or $S_2(N/O)_2$ coordination. The electronic absorption spectrum of Co(II)-SmtB is remarkably similar to Co(II),Zn-Zur (Figure 2). These observations suggest that the SmtB metal site is similar to site B in Zur. Furthermore, the Zn(II) affinity of SmtB was measured at greater than 10^{11} M^{-1} (*22*). This result parallels the extraordinary Zn(II) affinity measured for Zur (*6*). Spectroscopic characterization of these Zn(II) sensors is providing a greater understanding of the intracellular chemistry of this essential element.

ACKNOWLEDGMENT

We thank the staff of SSRL for making the X-ray absorption portion of this work possible. SSRL is supported by the Department of Energy, Office of Basic Energy Sciences, and the SSRL Biotechnology Program is supported by the National Institutes of Health, National Center for Research Resources, Biomedical Technology Program, and Department of Energy, Office of Biological and Environmental Research.

SUPPORTING INFORMATION AVAILABLE

Figure S1 showing fit statistics as a function of percent sulfur used in the fit for the zinc Zur data. This material is available free of charge via the Internet at http://pubs.acs.org.

REFERENCES

1. Brocklehurst, K. R., Hobman, J. L., Lawley, B., Blank, L., Marshall, S. J., Brown, N. L., and Morby, A. P. (1999) *Mol. Microbiol. 31*, 893−902.
2. Outten, C. E., Outten, F. W., and O'Halloran, T. V. (1999) *J. Biol. Chem. 274*, 37517−37524.
3. Binet, M. R., and Poole, R. K. (2000) *FEBS Lett. 473*, 67−70.
4. Patzer, S. I., and Hantke, K. (1998) *Mol. Microbiol. 28*, 1199−1210.
5. Patzer, S. I., and Hantke, K. (2000) *J. Biol. Chem. 275*, 24321−24332.
6. Outten, C. E., and O'Halloran, T. V. (2001) *Science 292*, 2488−2492.
7. Althaus, E. W., Outten, C. E., Olson, K. E., Cao, H., and O'Halloran, T. V. (1999) *Biochemistry 38*, 6559−6569.
8. Gonzalez de Peredo, A., Saint-Pierre, C., Adrait, A., Jacquamet, L., Latour, J. M., Michaud-Soret, I., and Forest, E. (1999) *Biochemistry 38*, 8582−8589.
9. Jacquamet, L., Dole, F., Jeandey, C., Oddou, J.-L., Perret, E., Le Pape, L., Aberdam, D., Hazemann, J.-L., Michaud-Soret, I., and Latour, J.-M. (2000) *J. Am. Chem. Soc. 122*, 394−395.
10. Bavoso, A., Ostuni, A., Battistuzzi, G., Menabue, L., Saladini, M., and Sola, M. (1998) *Biochem. Biophys. Res. Commun. 242*, 385−389.
11. Berkovits, H. J., and Berg, J. M. (1999) *Biochemistry 38*, 16826−16830.
12. Mely, Y., De Rocquigny, H., Morellet, N., Roques, B. P., and Gerad, D. (1996) *Biochemistry 35*, 5175−5182.
13. Roehm, P. C., and Berg, J. M. (1997) *Biochemistry 36*, 10240−10245.
14. McLendon, G., Hull, H., Larkin, K., and Chang, W. (1999) *J. Biol. Inorg. Chem. 4*, 171−174.
15. Maniatis, T., Fritsch, E. F., and Sambrook, J. (1982) *Molecular Cloning: A Laboratory Manual*, Cold Spring Harbor Laboratory Press, Cold Spring Harbor, NY.
16. Gill, S. C., and von Hippel, P. H. (1989) *Anal. Biochem. 182*, 319−326.
17. Clark-Baldwin, K., Tierney, D. L., Govindaswamy, N., Gruff, E. S., Kim, C., Berg, J., Koch, S. A., and Penner-Hahn, J. E. (1998) *J. Am. Chem. Soc. 120*, 8401−8409.
18. Rehr, J. J., Mustre de Leon, J., Zabinsky, S. I., and Albers, R. C. (1991) *J. Am. Chem. Soc. 113*, 5135−5140.
19. Bertini, I., and Luchinat, C. (1984) *Adv. Inorg. Biochem. 6*, 71−111.
20. Maret, W., and Vallee, B. L. (1993) *Methods Enzymol. 226*, 52−71.
21. Salowe, S. P., Marcy, A. I., Cuca, G. C., Smith, C. K., Kopka, I. E., Hagmann, W. K., and Hermes, J. D. (1992) *Biochemistry 31*, 4535−4540.
22. VanZile, M. L., Cosper, N. J., Scott, R. A., and Giedroc, D. P. (2000) *Biochemistry 39*, 11818−11829.
23. May, S. W., and Kuo, J. Y. (1978) *Biochemistry 17*, 3333−3338.
24. Vasak, M., Kagi, J. H., Holmquist, B., and Vallee, B. L. (1981) *Biochemistry 20*, 6659−6664.
25. Griep, M. A., Adkins, B. J., Hromas, D., Johnson, S., and Miller, J. (1997) *Biochemistry 36*, 544−553.
26. Brown, I. D., and Altermatt, D. (1985) *Acta Crystallogr. B41*, 244−247.
27. Tsang, H. T., Batie, C. J., Ballou, D. P., and Penner-Hahn, J. E. (1996) *J. Biol. Inorg. Chem. 1*, 24−33.
28. Jacquamet, L., Aberdam, D., Adrait, A., Hazemann, J. L., Latour, J. M., and Michaud-Soret, I. (1998) *Biochemistry 37*, 2564−2571.
29. Robinson, N. J., Bird, A. J., and Turner, J. S. (1998) in *Metal Ions in Gene Regulation* (Silver, S., and Walden, W., Eds.) pp 372−397, Chapman and Hall, New York.

BI0155448